Probing the fourth generation Majorana neutrino dark matter

Yu-Feng Zhou[*]

Kavli Institute for Theoretical Physics China,
State Key Laboratory of Theoretical Physics,
Institute of Theoretical Physics, Chinese Academy of Sciences
Beijing, 100190, P.R. China

Abstract

Heavy fourth generation Majorana neutrino can be stable and contribute to a small fraction of the relic density of dark matter (DM) in the Universe. Due to its strong coupling to the standard model particles, it can be probed by the current direct and indirect DM detection experiments even it is a subdominant component of the whole halo DM. Assuming that it contributes to the same fraction of the local halo DM density as that of the DM relic density in the Universe, we show that the current Xenon100 data constrain the mass of the stable Majorana neutrino to be greater than the mass of the top quark. In the mass range from 200 GeV to a few hundred GeV, the effective spin-independent cross section for the neutrino elastic scattering off nucleon is insensitive to the neutrino mass and mixing, and is predicted to be $\sim 1.5 \times 10^{-44}$ cm^2, which can be reached by the direct DM detection experiments soon. In the same mass region the predicted effective spin-dependent cross section for the heavy neutrino scattering off proton is in the range of 2×10^{-40} cm$^2 \sim 2 \times 10^{-39}$ cm^2, which is within the reach of the ongoing DM indirect search experiments such as IceCube. We demonstrate such properties of the heavy neutrino DM in a fourth generation model with the stability of the fourth Majorana neutrino protected by an additional generation-dependent $U(1)$ gauge symmetry.

---

[*]Email: yfzhou@itp.ac.cn

1 Introduction

Models with chiral fourth generation fermions are among the simplest and well-motivated extensions of the standard model (SM) and have been extensively studied [1]. The condition for CP symmetry violation in the SM requires at least three generations of fermions [2]. However, there is no upper limit on the number of generations from the first principle. In the SM the amount of CP violation is not large enough to explain the baryon-antibaryon asymmetry in the Universe. The inclusion of fourth generation quarks leads to two extra CP phases in quark sector and possible larger CP violation [3], which is helpful for electroweak baryogenesis. With very massive quarks in the fourth generation, it has been proposed that the electroweak symmetry breaking may become a dynamical feature of the SM [4–7].

The recent LHC and Tevatron experiments have imposed constraints on the mass of the fourth generation quarks from possible pair production processes. For instance, the lower limit on the mass of the fourth generation up-type quark u_4 is found to be $m_{u_4} \geq 450$ GeV from the search for the process $u_4 \bar{u}_4 \to Wb W\bar{b} \to b3j\ell^\pm \not{E}_T$, and the limit on the mass of the fourth generation down-type quark d_4 is $m_{d_4} \geq 490$ GeV from the process $d_4 \bar{d}_4 \to WtW\bar{t} \to \ell^\pm \ell^\pm b3j \not{E}_T$ [8]. The direct searches for extra quarks at Tevatron have set lower limits on the masses of u_4 to be $m_{u4} \geq 335$ GeV, with the assumption that the mass splitting between u_4 and the fourth generation down quark d_4 is smaller than the W mass and the branching ratio of $u_4 \to Wq$ is 100% [9]. The lower limit for the mass of d_4 is $m_{d4} \geq 385$ GeV from the search for $d_4 \to Wt$ and the search for $4W$ final states from the pair production of $p\bar{p} \to d_4 \bar{d}_4$ [10], with the assumption that $m_{u4} > m_{d4}$. Note that these limits are obtained with the assumptions of maximum mixing between the fourth and the third generation quarks and 100% branching ratio of the decay processes. The limits can be significantly weaker in models with suppressed mixing and decay branching ratio.

In fourth generation models, the production of the Higgs boson can be enhanced by a factor of 5-9 due to the presence of two additional fourth generation quarks in the one-loop gluon-gluon fusion process. In a combined analysis of ATLAS and CMS, the mass of the Higgs boson h^0 has been excluded in the range 120-600 GeV which is based on the searches for $h^0 \to \gamma\gamma$, $W^\pm W^\mp(W^{*\mp})$ and $Z^0 Z^0(Z^{*0})$ in fourth generation models [11]. In obtaining such a bound, it is assumed that the fourth generation fermions are heavy and do not contribute to the total width of the Higgs boson. Note that for a Higgs boson heavier than 600 GeV, the self-interaction of the Higgs boson may be very strong and even nonperturbative, while a Higgs boson lighter than 120 GeV may cause the problem of vacuum instability if the SM with fourth generation is valid up to the Planck scale.

The constraints on the masses of the fourth generation leptons are much weaker. The current lower bound on the mass of the unstable fourth generation charged lepton e_4 is $m_{e4} \geq 100.8$ GeV from the search for e_4 decaying into the fourth generation neutrino ν_4 and $W^\pm$ boson. From the invisible width of Z^0 boson, the lower bounds for the mass of an unstable ν_4 is set to be $m_{\nu4} \geq (101.3, 101.5, 90.3)$ GeV from the decay $\nu_4 \to (e, \mu, \tau) W^\pm$ in the case that ν_4 is of Dirac type. If ν_4 is of Majorana type the corresponding bounds are modified to be $m_{\nu4} \geq (89.5, 90.7, 80.5)$ GeV. The constraints are much weaker if ν_4 is a long-lived or stable particle. In this case the lower bound is around $\sim m_Z/2$: $m_{\nu4} \geq 45.0(39.5)$ GeV for Dirac (Majorana) neutrino [12]. A long-lived fourth neutrino can also relax the constraints from the precision electroweak data [13]. If the fourth generation neutrino is stable, it can be a potential candidate for the dark matter (DM) in the Universe.

Heavy stable neutrinos with mass greater than ~ 1 GeV are possible candidates for the cold DM [14,15]. However, if the neutrino is the dominant component of the halo DM, the current DM direct search experiments have imposed strong constraints on its mass. For instance, it has been shown that the spin-independent (SI) cross sections for the stable Dirac neutrino elastic scattering off nucleus can be a few order of magnitudes larger than the current DM direct search upper bounds due to the Z^0 and h^0 exchanges [16–19]. In the case of Majorana neutrino, the spin-dependent (SD) cross sections for the elastic scattering can be very large. Previous analysis based on the assumption that the Majorana neutrino dominates the local halo DM density have ruled out the mass range 10 GeV $- 2$ TeV from the upper bounds on the SD cross section [20]. The mass of the Majorana neutrino is also constrained from SI scattering through h^0-exchange if it has both Dirac and Majorana mass terms in the flavor basis [21]. On the other hand, it is well-known that for a neutrino heavier than $\sim m_Z/2$, the cross section for its annihilation is in general too large to reproduce the observed DM relic density. If the heavy neutrino mass is in the range $m_Z/2 \lesssim m_{\nu4} \lesssim m_W$, the annihilation into light fermion pairs $f\bar{f}$ through s-channel Z^0 exchange contributes to a very large cross section. For the neutrino heavier than m_W, the contribution from $f\bar{f}$ channels decrease rapidly. However, other channels such as $W^\pm W^\mp$, $Z^0 h^0$ etc. are opened. For these processes the corresponding cross section does not decrease with the increasing of the neutrino mass, resulting in a relic density always decreases with the growing of the neutrino mass, and a thermal relic density far below the observed total DM relic density [22]. Since the neutrino DM can only contribute to a small fraction of the relic density of DM, it is expected that it contributes to a small fraction of the halo DM density as well, and the two fractions are of the same order of magnitude. From model building point of view, it is easy to construct multi-component DM models with the heavy neutrino being a subdominant component

in the halo. Despite its very low number density in the halo, it can still be probed by the underground DM direct detection experiments due to its strong coupling to the target nuclei, which provides a way to search for new physics beyond the SM complementary to the LHC. In this case, the event rate of the DM-nucleus elastic scattering will depend on both the relic density and the cross section for the elastic scattering process. Since both of them have nontrivial dependence on the neutrino mass, the above mentioned constraints on the neutrino DM could be modified significantly.

In this work, we explore the consequence of this possibility in a model with a fourth generation Majorana neutrino DM. The stability of the fourth Majorana neutrino protected by an additional generation-dependent $U(1)$ gauge symmetry. In the model the gauge-anomalies generated by the first three generation fermions are canceled by the ones from the fourth generation. We perform an updated analysis of the Majorana neutrino DM in light of the recent Higgs search results at the LHC and the recent DM direct detection results such as Xenon100 and SIMPLE etc.. The relic density of the neutrino DM is obtained by calculating the annihilation cross sections for all the possible final states such as $f\bar{f}$, $W^{\pm}W^{\mp}$, Z^0Z^0, Z^0h^0 and h^0h^0 etc.. Under the assumption that the neutrino contributes to the same fraction of the local halo DM density as that of DM relic density in the Universe, we calculate the effective DM-nucleus elastic scattering cross sections which are the cross sections rescaled by the fraction of the halo DM density contributed by the heavy Majorana neutrino. The results show that the current Xenon100 data constrain the mass of the Majorana neutrino to be greater than ~ 175 GeV. In the mass range from 200 GeV to a few hundred GeV, the spin-independent cross section for the neutrino elastic scattering off nucleon is predicted to be $\sim 1.5 \times 10^{-44}$ cm^2, which is insensitive to the neutrino mass and can be reached by the direct DM search experiments in the near future. In the same mass range the predicted spin-dependent cross section for neutrino proton scattering is in the range 2×10^{-40} cm^2 $\sim 2 \times 10^{-39}$ cm^2, which is within the reach of the ongoing IceCube experiment. Although the analysis is performed in a specific model, the results are valid for a wide range of models with heavy Majorana neutrino DM.

This paper is organized as follows, in section 2, we present the details of the model with stable fourth generation Majorana neutrino and the interactions relevant to the calculation of the relic density and DM-nucleus elastic scattering cross sections. In section 3, we calculate the relic density of Majorana neutrino DM. In section 4, we give the prediction for spin-independent and spin-dependent cross sections for the heavy neutrino elastic scattering off nucleon and compared them with the latest DM search experiments. Finally, we give the conclusions in section 5.

4

2 A model with stable fourth generation neutrino

In this work we consider a simple extension of the SM with a sequential fourth generation and an additional $U(1)_F$ gauge symmetry. The $U(1)$ extensions to the SM are well motivated from the point view of grand unification such as the $SO(10)$ and E_6 and have rich phenomenology [23] which can be reached by the on going LHC experiments. The flavor contents in the model are given by

$$q_{iL} = \begin{pmatrix} u_{iL} \\ d_{iL} \end{pmatrix}, \ \ell_{iL} = \begin{pmatrix} \nu_{iL} \\ e_{iL} \end{pmatrix}, \ u_{iR}, \ d_{iR}, \ \nu_{iR}, \ e_{iR} \ (i = 1, \ldots, 4). \tag{1}$$

All the fermions in the model are vector-like under the extra gauge interactions associated with $U(1)_F$. The $U(1)_F$ charges of the fermions could be generation-dependent. In order to evade the stringent constraints from the tree-level flavor changing neutral currents (FCNCs), the $U(1)_F$ charges Q_{qi} for the first three generation quarks are set to be the same, i.e. $Q_{qi} = Q_q$, $(i = 1, 2, 3)$ while $Q_{q4} = -3Q_q$ for the fourth generation quarks. Similarly, the $U(1)_F$ charges for the first three generation and the fourth generation leptons are Q_L and $-3Q_L$, respectively. In general, Q_q and Q_L can be different. For simplicity, in this work we take $Q_q = Q_L = 1$. With this set of flavor contents and $U(1)_F$ charge assignments, it is straight forward to see that the new gauge interactions are anomaly-free. Since the gauge interaction of $U(1)_F$ is vector-like, the triangle anomalies of $[U(1)_F]^3$, $[SU(3)_C]^2 U(1)_F$ and $[\text{gravity}]^2 U(1)_F$ are all vanishing. The anomaly of $U(1)_Y [U(1)_F]^2$ is zero because the $U(1)_Y$ hypercharges cancel for quarks and leptons separately in each generation, namely $\sum(-Y_{qL} + Y_{qR}) = 0$ and $\sum(-Y_{\ell L} + Y_{\ell R}) = 0$. The anomaly of $[SU(2)_L]^2 U(1)_F$ is also zero due to the relation

$$\sum_{i=1}^{4} Q_{qi} = 0 \quad \text{and} \quad \sum_{i=1}^{4} Q_{Li} = 0. \tag{2}$$

Thus in this model, the gauge anomalies generated by the first three generation fermions are canceled by that of the fourth generation one, which also gives a motivation for the inclusion of the fourth generation.

The gauge symmetry $U(1)_F$ is to be spontaneously broken by the Higgs mechanism. For this purpose we introduce two SM singlet scalar fields $\phi_{a,b}$ which carry the $U(1)_F$ charges $Q_a = -2Q_L$ and $Q_b = 6Q_L$ respectively. The $U(1)_F$ charges of $\phi_{a,b}$ are arranged such that ϕ_a can have Majorana type of Yukawa couplings to the right-handed neutrinos of the first three generations ν_{iR} $(i = 1, 2, 3)$ while ϕ_b only couples to the fourth generation neutrino ν_{4R}. After the spontaneous symmetry breaking, the two scalar fields obtain vacuum expectation values (VEVs) $\langle \phi_{a,b} \rangle = v_{a,b}/\sqrt{2}$.

The relevant interactions in the model are given by

$$
\begin{aligned}
\mathcal{L} = {} & \bar{f}_i i \gamma^\mu D_\mu f_i + (D_\mu \phi_a)^\dagger (D_\mu \phi_a) + (D_\mu \phi_b)^\dagger (D_\mu \phi_b) \\
& - Y^d_{ij} \bar{q}_{iL} H d_{iR} - Y^u_{ij} \bar{q}_{iL} \tilde{H} u_{iR} - Y^e_{ij} \bar{\ell}_{iL} H e_{iR} - Y^\nu_{ij} \bar{\ell}_{iL} \tilde{H} \nu_{iR} \\
& - \frac{1}{2} Y^m_{ij} \overline{\nu^c_{iR}} \phi_a \nu_{jR} \ (i,j=1,2,3) - \frac{1}{2} Y^m_4 \overline{\nu^c_{4R}} \phi_b \nu_{4R} - V(\phi_a, \phi_b, H) + \text{H.c.} \quad (3)
\end{aligned}
$$

where f_i stand for left- and right-handed fermions, and H is the SM Higgs doublet. $D_\mu f_i = (\partial_\mu - i g_1 \tau^a W^a_\mu - i Y g_2 B_\mu - i Q_f g_F Z'_\mu) f_i$ is the covariant derivative with Z'_μ the extra gauge boson associated with the $U(1)_F$ gauge symmetry, and g_F the corresponding gauge coupling constant. Since $\phi_{a,b}$ are SM singlets, they do not play any role in the electroweak symmetry breaking. Thus Z' obtains mass only from the VEVs of the scalars

$$
m^2_{Z'} = g^2_F (Q^2_a v^2_a + Q^2_b v^2_b), \quad (4)
$$

and it does not mix with Z^0 boson in mass term at tree level. It can only mix with Z^0 through kinetic mixing. In this work we assume that the effect of the kinetic mixing is small and negligible.

From the $U(1)_F$ charge assignments in the model, the four by four Yukawa coupling matrix is constrained to be of the block diagonal form $\mathbf{3} \otimes \mathbf{1}$ in the generation space. Since the $U(1)_F$ charges are the same for the fermions in the first three generation, there is no tree level FCNC induced by the Z'-exchange in the physical basis after diagonalization. Thus a number of constraints from the low energy flavor physics such as the neutral meson mixings and the $b \to s\gamma$ can be avoided.

The contribution to the muon $g-2$ from the Z' boson at one-loop can be estimated as [24]

$$
\Delta a_\mu \approx \frac{g^2_F}{12\pi^2} \frac{m^2_\mu}{m^2_{Z'}}. \quad (5)
$$

The current experimental data requires that $\Delta a_\mu \leq 3.9 \times 10^{-9}$ [25, 26], which can be translated into a lower bound on the VEVs of $\phi_{a,b}$: $\sqrt{Q^2_a v^2_a + Q^2_b v^2_b} \geq 1.45 \times 10^2$ GeV. Note that the dependence on the coupling constant g_F is canceled by the one in the mass of Z' in the expression of Δa_μ. The direct search for the process $e^+ e^- \to Z' \to \ell^+ \ell^-$ at the LEP-II leads to a lower bound on the ratio of the mass to the coupling to leptons: $M_{Z'}/g_F \geq 6$ TeV [27] for vector-like interactions, which corresponds to a more stringent lower bound: $\sqrt{Q^2_a v^2_a + Q^2_b v^2_b} \geq 6$ TeV.

The current searches for narrow resonances in the Drell-Yan process $pp \to Z' \to \ell^+ \ell^-$ at the LHC impose an alternative bound on the mass and the couplings of the Z' boson. In the narrow width approximation, the cross section for the Drell-Yan process can be

parametrized as $\sigma = (\pi/(48s))[c_u w_u(s, M_{Z'}^2) + c_d w_d(s, M_{Z'}^2)]$, where s is the squared center of mass energy and $w_{u,d}(s, M_{Z'}^2)$ are model-independent functions depending on $M_{Z'}$ [27]. The coefficients $c_{u,d}$ are related to the Z' couplings to the quarks as $c_q = g^2(Q_{qL}^2 + Q_{qR}^2)Br(Z' \to \ell^+\ell^-)$ $(q = u, d)$ where $Q_{qL,qR}$ are the charges of the left- and right-handed quarks of a generic $U(1)$ gauge symmetry with coupling strength g. The limit on the cross section reported by the experiments can be recast model-independently as limit contours in the $c_u - c_d$ plan with unique contour for each value of $M_{Z'}$ [27]. Using the $c_u - c_d$ contours, the limits on one type of Z' model can be translated into that of other models. For a model with sequential neutral gauge boson Z'_{SSM} which by definition has the same couplings as that for the SM Z^0 boson [23], the latest lower bounds on its mass $M_{Z'_{SSM}}$ is 1.94 TeV from CMS [28] and 1.83 TeV from ATLAS [29] respectively. In the Z'_{SSM} model $c_u^{SSM} \approx 2.36 \times 10^{-3}$ and $c_d^{SSM} \approx 3.66 \times 10^{-3}$. The bound on $M_{Z'_{SSM}}$ can be translated into the bound on the mass and couplings of the Z' in this model in which $c_u = c_d = 18g_F^2 Br(Z' \to \mu^+\mu^-)$. By requiring that $c_u \leq c_u^{SSM}$ at $M_{Z'} = 1.94$ TeV, we obtain $g_F \leq 0.051$. Numerical analyses have shown that for a given limit on the cross section, as the combination $c_u w_u + c_d w_d$ increases or decreases by an order of magnitude, the mass limit changes roughly by 500 GeV [30, 31]. Thus as a rough estimation one can obtain limits on g_F for other values of $M_{Z'}$, for instance $g_F \lesssim 0.029$ for $M_{Z'} = 1.44$ TeV and $g_F \lesssim 0.0051$ for $M_{Z'} = 0.94$ TeV, respectively.

In this model, there is no mixing between the fourth and the first three generation quarks, thus the null results in searching for $u_4 \to bW^\pm$ and $d_4 \to tW^\pm$ at the LHC do not impose constraints on the masses of u_4 and d_4. The model is not constrained by the FCNC processes $u_4 \to tX$ or $d_4 \to bX$ either [32].

The fourth generation neutrinos obtain both Dirac and Majorana mass terms through the vacuum expectation values (VEVs) of H and ϕ_b. In the basis of $(\nu_L, \nu_R^c)^T$ the mass matrix for the fourth neutrino is given by

$$m_\nu = \begin{pmatrix} 0 & m_D \\ m_D & m_M \end{pmatrix}, \tag{6}$$

where $m_D = Y_4^\nu v_H/\sqrt{2}$ with $v_H = 246$ GeV and $m_M = Y_4^m v_{\phi_b}/\sqrt{2}$. The left-handed components $(\nu_{1L}^{(m)}, \nu_{2L}^{(m)})$ of the two mass eigenstates are related to the ones in the flavor eigenstates by a rotation angle θ

$$\nu_{1L}^{(m)} = -i(c_\theta \nu_L - s_\theta \nu_R^c), \quad \nu_{2L}^{(m)} = s_\theta \nu_L + c_\theta \nu_R^c, \tag{7}$$

where $s_\theta \equiv \sin\theta$ and $c_\theta \equiv \cos\theta$. The value of θ is defined in the range $(0, \pi/4)$ and is determined by

$$\tan 2\theta = \frac{2m_D}{m_M}, \tag{8}$$

with $\theta = 0$ $(\pi/4)$ corresponding to the limit of minimal (maximal) mixing. The phase i is introduced to render the two mass eigenvalues real and positive. The two Majorana mass eigenstates are $\chi_1 = \nu_{1L}^{(m)} + \nu_{1L}^{(m)c}$ and $\chi_2 = \nu_{2L}^{(m)} + \nu_{2L}^{(m)c}$, respectively. The masses of the two neutrinos are given by $m_{1,2} = (\sqrt{m_M^2 + 4m_D^2} \mp m_M)/2$. In terms of the mixing angle θ they can be rewritten as

$$m_1 = \left(\frac{s_\theta}{c_\theta}\right) m_D, \quad \text{and} \quad m_2 = \left(\frac{c_\theta}{s_\theta}\right) m_D, \tag{9}$$

with $m_1 \leq m_2$. Note that for all the possible values of θ the lighter neutrino mass eigenstate χ_1 consists of more left-handed neutrino than the right-handed one, which means that χ_1 always has sizable coupling to the SM Z^0 boson. Therefore the LEP-II bound on the mass of stable neutrino is always valid for χ_1, which is insensitive to the mixing angle.

As the fermions in the first three generations and the fourth generation have different $U(1)_F$ charges, the fourth generation fermions cannot mix with the ones in the first three generations through Yukawa interactions. After the spontaneous breaking down of $U(1)_F$, there exists a residual Z_2 symmetry for the fourth generation fermions which protect the fourth neutrino χ_1 to be a stable particle if it is lighter than the fourth generation charged lepton e_4, which makes it a possible dark matter candidate.

Although the stability of χ_1 can be achieved easily by imposing an *ad hoc* Z_2 symmetry *only* on the fourth generation, it is theoretically more attractive to consider a Z_2 which originates from a $U(1)$ gauge symmetry in which all the fermions are charged. First, models with extra $U(1)$ gauge symmetries are well motivated from various GUT models such as $SO(10)$ and E_6 etc., and it is common to link a discrete Z_N symmetry to a broken continuous $U(1)$ symmetry in model building. Second, in this model all the four generations are treated in parallel, The only difference is the $U(1)$ charge of the fourth generation fermions. Due to this $U(1)$ charge difference, after the spontaneous symmetry breaking by the VEVs of ϕ_a and ϕ_b , the $U(1)$ is broken into two separate Z_2 symmetries, with one on the first three generation and the other one on the fourth generation which stabilizes the fourth generation neutrino. Third, in this model setup, all the fermions are vector-like under the extra $U(1)$ gauge interactions. The cancellation of gauge anomalies automatically requires the existence of the right-handed neutrinos in each generation. Thus in this model it is natural to have extra stable neutrinos.

In the mass basis the interaction between the massive neutrinos and the SM Z^0 boson is given by

$$\mathcal{L}_{NC} = \frac{g_1}{4\cos\theta_W} \left[-c_\theta^2 \bar\chi_1 \gamma^\mu \gamma^5 \chi_1 - s_\theta^2 \bar\chi_2 \gamma^\mu \gamma^5 \chi_2 + 2ic_\theta s_\theta \bar\chi_1 \gamma^\mu \chi_2 \right] Z_\mu, \tag{10}$$

where g_1 is the weak gauge coupling and θ_W is the Weinberg angle. The Yukawa interaction between $\chi_{1,2}$ and the SM Higgs boson is given by

$$\mathcal{L}_Y = -\frac{m_1}{v_H}\left(\frac{c_\theta}{s_\theta}\right)\left[c_\theta s_\theta\bar{\chi}_1\chi_1 + c_\theta s_\theta\bar{\chi}_2\chi_2 - i(c_\theta^2 - s_\theta^2)\bar{\chi}_1\gamma^5\chi_2\right]h^0. \tag{11}$$

Since all the fermions are vector-like under the $U(1)_F$ gauge interaction and $\chi_{1,2}$ are neutral particles, only the off-diagonal interaction $\bar{\chi}_1\chi_2 Z'$ is allowed.

3   Annihilation cross sections and relic density of the fourth generation neutrino dark matter

The thermal relic density of χ_1 is related to its annihilation cross section at freeze out. The Feynman diagrams for all possible annihilation channels are shown in Fig. 1. When the mass of χ_1 is smaller than that of the $W^\pm$ boson, $\chi_1\chi_1$ can only annihilate into light SM fermion pairs through s-channel Z^0/h^0 exchange. For Majorana neutrino the annihilation cross sections are suppressed by the small masses of the final state fermions. However, large enhancement of the annihilation cross section occurs if the mass of χ_1 is close to $m_Z/2$ such that the intermediate Z^0 is nearly on shell. When the fourth generation neutrino is heavier than the $W^\pm$ boson, the $W^\pm W^\mp$ channel will open and become important. The process $\chi_1\chi_1 \to W^\pm W^\mp$ involves s-channel Z^0 and h^0 boson exchange and t-channel e_4 exchange. All these three intermediate states must be included in order to maintain the unitarity. For even heavier χ_1, the final states can be Z^0Z^0, Z^0h^0 and h^0h^0. The Z^0Z^0 channel contains the process of s-channel h^0 exchange and the t-channel $\chi_{1,2}$ exchange. Similarly, the Z^0h^0 channel contains s-channel Z^0 exchange and the t-channel $\chi_{1,2}$ exchange processes. The h^0h^0 channel is dominated by the t-channel processes due to the large Yukawa coupling. When χ_1 is heavier than the top quark, the $\bar{t}t$ final states must be included. The cross section can be large as the top quark has large Yukawa couplings to the Higgs boson. In this work we neglect the $Z'Z'$ final states by assuming that Z' is always heavier than χ_1.

We numerically calculate the cross sections for $\chi_1\chi_1$ annihilation into all the relevant final states using CalHEP 2.4 [33]. In order to determine the DM relic density, one needs to calculate the thermally averaged product of the DM annihilation cross section and the relative velocity

$$\langle\sigma v\rangle = \frac{1}{8m_1^2TK_2^2(m_1/T)}\int_{4m_1^2}^{\infty}ds\sigma(s-4m_1^2)\sqrt{s}K_1\left(\frac{\sqrt{s}}{T}\right), \tag{12}$$

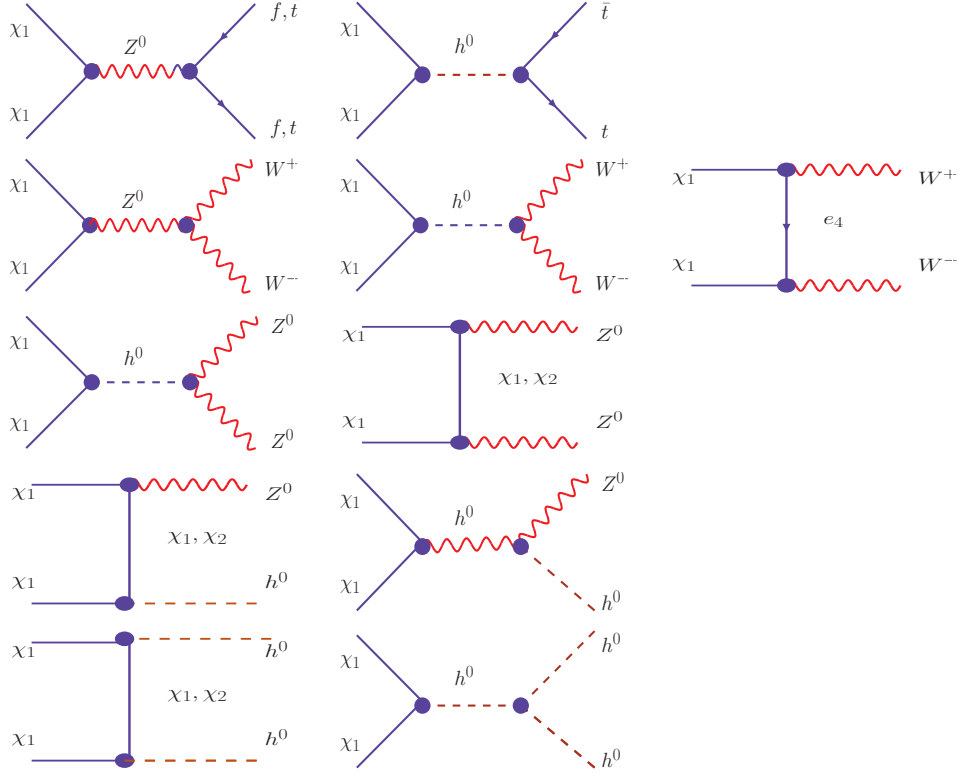where T is temperature and $K_{1,2}(x)$ are the modified Bessel function of the second kind.

Figure 1: Feynman diagrams for $\chi_1\chi_1$ annihilating into SM particles $\bar{f}f$, $\bar{t}t$, $W^{\pm}W^{\mp}$, Z^0Z^0, Z^0h^0 and h^0h^0.

The relic abundance can be approximated by

$$\Omega h^2 \simeq \frac{1.07 \times 10^9 \text{GeV}^{-1}}{\sqrt{g_*}M_{pl}\int_{x_F}^{\infty}\frac{\langle\sigma v\rangle}{x^2}dx}, \tag{13}$$

where $x = m_1/T$ is the rescaled inverse temperature. $x_F \approx 25$ corresponds to the decoupling temperature, $g_* = 86.25$ is the number of effective relativistic degree of freedom at the time of freeze out, and $M_{pl} = 1.22 \times 10^{19}$ GeV is the Planck mass scale.

In the left panel of Fig. 2, we show the value of $\langle\sigma v\rangle$ at the time of freeze out $x_F = 25$ as function of m_1. In the figure, the contributions from individual final states are also given. The peak at $m_\chi \simeq m_Z/2$ corresponds to the case of resonant s-channel annihilation when the intermediate Z^0 boson is nearly on shell. During the numerical calculations the mass difference between the charged fourth generation lepton e_4 and χ_1 is set to be $m_{e_4} - m_{\chi_1} = 50$ GeV. Note that a very large mass difference is subject to strong constraints from the electroweak precision data [34]. The results are found to be insensitive to the mass difference. In the left panel of Fig. 2 the mixing angle θ is fixed at 30°. The recent LHC experiments have placed strong constraints on the mass of h^0. For the fourth generation model the mass of h^0 is constrained to be below 120 GeV

10

or heavier than 600 GeV [11]. In the numerical calculations the mass of the SM Higgs boson h^0 is fixed at 115 GeV.

In the case that the Higgs boson is light enough to be among the final states of the $\chi_1\chi_1$ annihilation, the contributions from the Z^0h^0 and h^0h^0 final states can be important. It has already been noticed that the Z^0h^0 channel can be as importance as the $W^\pm W^\mp$ channel in the case of heavy Dirac neutrino DM [19]. In the Majorana case, since the $W^\pm W^\mp$ cross section is strongly suppressed by the smallness of the relative velocity [35], the Z^0h^0 channel can give the dominant contribution to the cross section.

In the right panel of Fig. 2, we show the quantity

$$r_\Omega \equiv \frac{\Omega_{\chi_1}}{\Omega_{DM}}, \tag{14}$$

which is the ratio of the relic density of χ_1 to the observed total DM relic density $\Omega_{DM}h^2 = 0.110 \pm 0.006$ [12] as function of the mass of χ_1 for different values of the mixing angle θ. The results show a significant dependence on the mixing angle θ. For smaller mixing angle θ the couplings between χ_1 and gauge bosons $W^\pm, Z$ are stronger, resulting in a smaller relic density. The results also clearly show that due to the large annihilation cross section, χ_1 cannot make up the whole DM in the Universe. χ_1 can contribute to $\sim 20-40\%$ of the total DM relic density when its mass is around 80 GeV. But for $m_1 \gtrsim m_t$, it can contribute only a few percent or less to the whole DM.

However, since χ_1 has strong couplings to h^0 and Z^0, even in the case that the number density of χ_1 is very low in the DM halo, it is still possible that it can be detected by its elastic scattering off nucleus in direct detection experiments. Given the difficulties in detecting such a neutral and stable particle at the LHC, there is a possibility that the stable fourth generation neutrino could be first seen at the DM direct detection experiments.

In this model there exists three right-handed neutrinos v_{iR} ($i = 1, 2, 3$) in the first three generations. In the physical basis there may exist three sterile neutrinos, provided that the mixings between the left- and right-handed neutrinos are tiny. If one of the sterile neutrinos has a mass around keV scale, it can be a good candidate for warm dark matter which could be the dominant component of the DM in the Universe. The warm dark matter may provide a solution to some of the known problems in the DM simulations based on cold DM, such as reducing the number of subhalos and smoothing the cusps in the DM halo center. In the SM with only right-handed neutrinos, the sterile neutrino may obtain the correct relic density through non-thermal production [36]. In this model, since the keV sterile neutrino can annihilate into the light active neutrinos through the extra $U(1)_F$ gauge interactions, it can also be a thermal relic. In this case, the correct relic density can be obtained by including the effect of entropy dilution through the decays of other heavier sterile neutrinos [37].
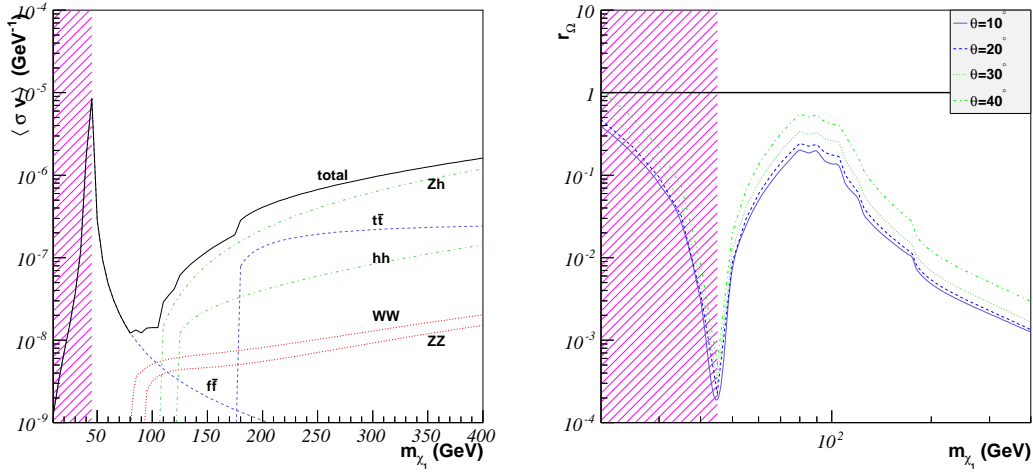
Figure 2: Left) Thermally averaged product of the annihilation cross section and the relative velocity as function of the mass of the stable heavy neutrino χ_1. The contributions from individual final states are also shown; right) the rescaled χ_1 relic density r_Ω as function of the mass of χ_1. The shaded region is excluded by the LEP-II experiments.

4 Direct detections of the fourth generation neutrino dark matter

The generic formula for the differential event rate of DM-nucleus scattering per nucleus mass is given by

$$
\frac{dN}{dE_R} = \frac{\rho_{DM}\sigma_N}{2m_{DM}\mu_N^2}F^2(E_R)\int_{v_{min}}^{v_{esc}} d^3v \frac{f(v)}{v}, \tag{15}
$$

where E_R is the recoil energy, σ_N is the scattering cross section corresponding to the zero momentum transfer, m_{DM} is the mass of the DM particle, $\mu_N = m_{DM}m_N/(m_{DM}+m_N)$ is the DM-nucleus reduced mass, $F(E_R)$ is the form factor, and $f(v)$ is the velocity distribution function of the halo DM. The local DM density ρ_{DM} is often set to be equal to $\rho_0 \simeq 0.3$ GeV/cm^3 (for updated determinations of ρ_0 see e.g. [38]) which is the local DM density inferred from astrophysics based on a smooth halo profile. Since the neutrino DM can only contribute to a small fraction of the relic density of DM, it is likely that it also contributes to a small fraction of the halo DM density, namely, its local density ρ_1 is much smaller than ρ_0. If the DM particles are nearly collisionless and there is no long range interactions which are different for different DM components, the structure formation process should not change the relative abundances of the DM components. In this work, we assume that ρ_1 is proportional to the relic density of χ_1 in the Universe,

namely

$$r_\rho \equiv \frac{\rho_1}{\rho_0} \approx \frac{\Omega_{\chi_1}}{\Omega_{DM}},$$ (16)

or $r_\rho \approx r_\Omega$. Consequently, the expected event rates of the DM-nucleus elastic scattering will be scaled down by r_ρ. In order to directly compare the theoretical predictions with the reported experimental upper limits which are often obtained under the assumption that the local DM particle density is ρ_0, we shall calculate the rescaled elastic scattering cross section

$$\tilde{\sigma} \equiv r_\rho \sigma \approx r_\Omega \sigma,$$ (17)

which corresponds to the event rate to be seen at the direct detection experiments. Note that $\tilde{\sigma}$ depends on the mass of χ_1 through the ratio r_ρ even when σ is mass-independent.

The spin-independent DM-nucleon elastic scattering cross section in the limit of zero momentum transfer is given by [39]

$$\sigma_n^{SI} = \frac{4\mu_n^2}{\pi} \frac{[Zf_p + (A-Z)f_n]^2}{A^2},$$ (18)

where Z and $A - Z$ are the number of protons and neutrons within the target nucleus, respectively. $\mu_n = m_1 m_n/(m_1 + m_n)$ is the DM-nucleon reduced mass. The coupling between DM and the proton (neutron) is given by

$$f_{p(n)} = \sum_{q=u,d,s} f_{Tq}^{p(n)} a_q \frac{m_{p(n)}}{m_q} + \frac{2}{27} f_{TG}^{p(n)} \sum_{q=c,b,t} a_q \frac{m_{p(n)}}{m_q},$$ (19)

with $f_{Tq}^{p(n)}$ the DM coupling to light quarks and $f_{TG}^{p(n)} = 1 - \sum_{q=u,d,s} f_{Tq}^{p(n)}$. In the case that the elastic scattering is dominated by t-channel Higgs boson exchange, the relation $f_n \simeq f_p$ holds and one has $\sigma_n^{SI} \simeq 4f_n^2\mu_n^2/\pi$. In numerical calculations we take $f_{Tu}^p = 0.020 \pm 0.004$, $f_{Td}^p = 0.026 \pm 0.005$, $f_{Ts}^p = 0.118 \pm 0.062$, $f_{Tu}^n = 0.014 \pm 0.003$, $f_{Td}^n = 0.036 \pm 0.008$ and $f_{Ts}^n = 0.118 \pm 0.062$ [40]. The coefficient a_q in the model is given by

$$a_q = c_\theta^2 \frac{m_1 m_q}{v_H^2 m_h^2}.$$ (20)

The value of a_q is proportional to m_1, thus larger elastic scattering cross section is expected for heavier χ_1. Note that in terms of m_1 the coefficient a_q is proportional to c_θ^2. Part of the mixing effects has been absorbed into the mass of χ_1. In the limit of $\theta \to 0$, m_1 is approaching zero and the couping between χ_1 and h^0 is vanishing as expected. The value of a_q has a strong dependence on m_h. As the latest LHC data exclude the mass of h^0 in the range 120 GeV-600 GeV in the presence of fourth generation fermions [11], we fix $m_h = 115$ GeV in the numerical calculations. The quark mass m_q in the expression

of a_q cancels the one in the expression of $f_{p(n)}$. Thus there is no quark mass dependence in the calculations.

In Fig. 3 we give the predicted spin-independent effective cross sections $\tilde{\sigma}_n^{SI}$ for the fourth generation neutrino elastic scattering off nucleon as function of its mass for different values of the mixing angle θ. One sees that even after the inclusion of the rescaling factor r_ρ, the current Xenon100 data can still rule out a stable fourth generation neutrino in the mass range $55\,\text{GeV} \lesssim m_1 \lesssim 175\,\text{GeV}$ which corresponds to $r_\Omega \lesssim 1\%$. Thus the stable fourth generation neutrino must be heavier than the top quark, and can only contribute to a small fraction of the total DM relic density

On the other hand, for $m_{\chi_1} \gtrsim 200\,\text{GeV}$, the cross section does not decrease with m_{χ_1} increasing, and is nearly a constant $\tilde{\sigma}_n^{SI} \approx 1.5 \times 10^{-44}\text{cm}^2$ in the range $200\,\text{GeV} \lesssim m_{\chi_1} \lesssim 400\,\text{GeV}$. This is due to the enhanced Yukawa coupling between the fourth generation neutrino and the Higgs boson which is proportional to m_{χ_1}, as it is shown in the expression of a_q. One can see from the Fig. 3 that the result is not sensitive to the mixing angle θ either, which is due to the compensation of the similar dependencies on θ in the relic density. For instance, the cross sections for the $W^\pm W^\mp$ and $Z^0 Z^0$ channel of $\chi\chi$ annihilation are proportional to c_θ^4, which compensates the θ-dependence in the a_q for the elastic scattering processes.

The Majorana neutrino DM can contribute to spin-dependent elastic scattering cross section through axial-vector interaction induced by the exchange of the Z^0 boson. At zero momentum transfer, the spin-dependent cross section has the following form [39]

$$\sigma_N^{SD} = \frac{32}{\pi} G_F^2 \mu_n^2 \frac{J+1}{J} \left(a_p \langle S_p \rangle + a_n \langle S_n \rangle \right)^2 , \tag{21}$$

where J is the spin of the nucleus, $a_{p(n)}$ is the DM effective coupling to proton (neutron) and $\langle S_{p(n)} \rangle$ the expectation value of the spin content of the nucleon within the nucleus. G_F is the Fermi constant. The coupling $a_{p(n)}$ can be written as

$$a_{p(n)} = \sum_{u,d,s} \frac{d_q}{\sqrt{2}G_F} \Delta_q^{p(n)}, \tag{22}$$

where d_q is the DM coupling to quark and $\Delta_q^{p(n)}$ is the fraction of the proton (neutron) spin carried by a given quark q. The spin-dependent DM-nucleon elastic scattering cross section is given by

$$\sigma_{p(n)}^{SD} = \frac{24}{\pi} G_F^2 \mu_n^2 \left(\frac{d_u}{\sqrt{2}G_F} \Delta_u^{p(n)} + \frac{d_d}{\sqrt{2}G_F} \Delta_d^{p(n)} + \frac{d_s}{\sqrt{2}G_F} \Delta_s^{p(n)} \right)^2 . \tag{23}$$

In numerical calculations we take $\Delta_u^p = 0.77$, $\Delta_d^p = -0.40$, $\Delta_s^p = -0.12$ [43], and use the relations $\Delta_u^n = \Delta_d^p$, $\Delta_d^n = \Delta_u^p$, $\Delta_s^n = \Delta_s^p$. The coefficients d_q in this model are given by

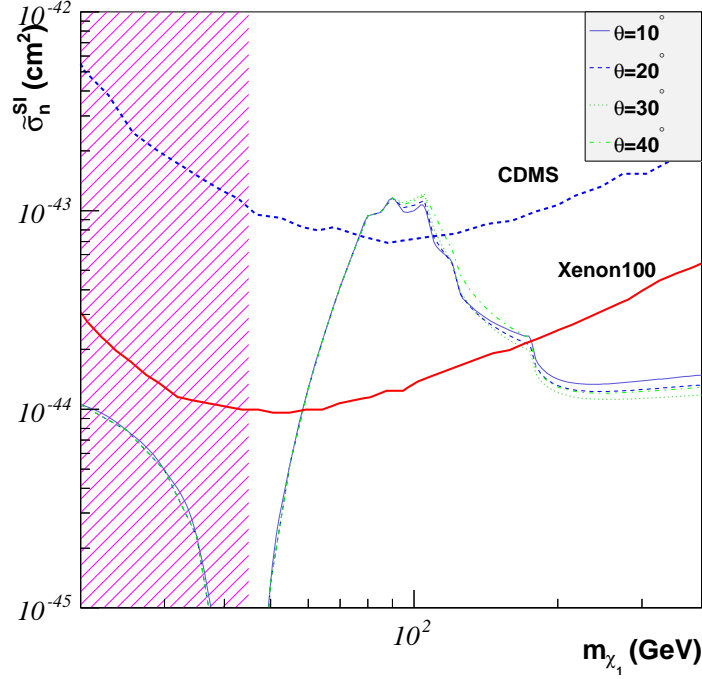$$d_u = -d_d = -d_s = \frac{G_F}{\sqrt{2}}. \tag{24}$$

14

Figure 3: Effective spin-independent cross section $\tilde{\sigma}_n^{SI}$ which is σ_n^{SI} rescaled by $r_\rho \approx r_\Omega$ for χ_1 elastically scattering off nucleon as function of the mass of χ_1. Four curves correspond to the mixing angle $\theta = 10°$(solid), $20°$(dashed), $30°$(dotted) and $40°$(dot-dashed) respectively. The current upper limits from CDMS [41] and Xenon100 [42] experiments are also shown.

For the axial-vector interactions, the coupling strengths do not depend on the electromagnetic charges of the quarks.

In Fig. 4 we show the predicted effective spin-dependent DM-neutron cross section $\tilde{\sigma}_n^{SD}$ as function of the neutrino mass for different mixing angles, together with various experimental upper limits. Since σ_n^{SD} is independent of m_{χ_1}, the dependency of $\tilde{\sigma}_{p(n)}^{SD}$ on the neutrino mass comes from the dependency of r_ρ on m_{χ_1}, which can be seen by comparing Fig. 4 with Fig. 2. The Xenon10 data is able to exclude the neutrino DM in the mass range $60\,\mathrm{GeV} \lesssim m_{\chi_1} \lesssim 120\,\mathrm{GeV}$, which is not as strong as that from the Xenon100 data on spin-independent elastic scattering cross section. For a heavy neutrino DM with mass in the range $200\,\mathrm{GeV} \lesssim m_{\chi_1} \lesssim 400\,\mathrm{GeV}$ the predicted spin-dependent cross section is between $10^{-40}\,\mathrm{cm}^2$ and $10^{-39}\,\mathrm{cm}^2$.

In Fig. 5 we give the predicted spin-dependent DM-proton cross section $\tilde{\sigma}_p^{SD}$. The cross sections for Majorana neutrino DM scattering off proton and neutron are quite similar, which is due to the fact that the relative opposite signs in Δ_u and Δ_d are

15

compensated by the opposite signs in d_u and d_n. So far the most stringent limit on the DM-proton spin-dependent cross section is reported by the SIMPLE experiment [44]. The SIMPLE result is able to exclude the mass range 50 GeV $\lesssim m_{\chi_1} \lesssim$ 150 GeV, which is compatible with the constraints from Xenon100. In Fig. 5, we also show the upper limits from indirect searches using up-going muons which are related to the annihilation of stable fourth generation neutrinos captured in the Sun. The limit from the Super-K experiment is obtained with the assumption that 80% of the DM annihilation products are from $b\bar{b}$, 10% from $c\bar{c}$ and 10% from $\tau\bar{\tau}$ respectively [45]. In the range 170 GeV $\lesssim m_{\chi_1} \lesssim$ 400 GeV, the limit from Super-K is $\sim 5 \times 10^{-39}$ cm^2. The IceCube sets a stronger limit $\tilde{\sigma}_p^{SD} \leq 2 \times 10^{-40}$ cm^2 for the DM mass at 250 GeV [46]. This limit is obtained with the assumption that the DM annihilation products are dominated by $W^{\pm}W^{\mp}$. If the annihilation products are dominated by $b\bar{b}$, the limit is much weaker, for instance $\tilde{\sigma}_p^{SD} \leq 5 \times 10^{-38}$ cm^2 for the DM mass at 500 GeV [46]. Note that in this model, the dominant final state is $Z^0 h^0$. The expected limit should be somewhere in between. Nevertheless, the IceCube has the potential to test the predictions in this model.

Different assumptions on the value of r_ρ and the nature of the heavy stable neutrino may result in different limits. For instance, in Ref. [20], an excluded mass range of 10 GeV-2 TeV is obtained from the Xenon 10 data on the cross section of the spin-dependent DM-nucleus elastic scattering, which is based on the assumption that the local halo DM is entirely composed of stable Majorana neutrino, i.e. $r_\rho = 1$, and the neutrino has the same couplings to the Z^0 boson as that of the SM active neutrinos. As in the present model we have $r_\rho \approx r_\Omega \ll 1$ and the coupling to the Z^0 boson depends on the mixing angle, the resulting constraints are different significantly.

5   Conclusions

In conclusion, we have investigated the properties of stable fourth generation Majorana neutrinos as dark matter particles. Although they contribute to a small fraction of the whole DM in the Universe, they can still be easily probed by the current direct detection experiments due to their strong couplings to the SM particles. We have considered a fourth generation model with the stability of the fourth Majorana neutrino protected by an additional generation-dependent $U(1)$ gauge symmetry. In the model the gauge-anomalies generated by the first three generation fermions are canceled by the ones from the fourth generation. We have shown that the current Xenon100 data constrain the mass of the stable Majorana neutrino to be greater than the mass of the top quark. For a stable Majorana neutrino heavier than the top quark, the effective spin-independent cross section for the elastic scattering off nucleon is found to be insensitive to the neutrino mass
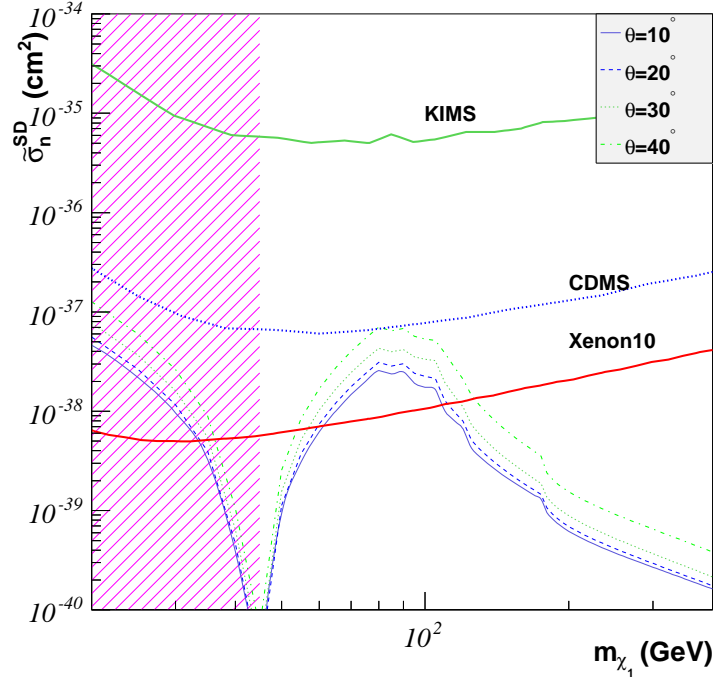
Figure 4: Effective spin-dependent cross section $\tilde{\sigma}_n^{SD}$ which is σ_n^{SD} rescaled by $r_\rho \approx r_\Omega$ for χ_1 elastically scattering off neutron as function of the mass of χ_1. Four curves correspond to the mixing angle $\theta = 10°$(solid), $20°$(dashed), $30°$(dotted) and $40°$(dot-dashed) respectively. The current upper limits from various experiments such as KIMS [47], CDMS [48] and Xenon10 [20] are also shown.

and is predicted to be around 10^{-44} cm^2, which can be reached by the direct DM search experiments in the near future. The predicted effective spin-dependent cross section for the heavy neutrino scattering off proton is in the range 10^{-40} cm$^2 \sim 10^{-39}$ cm^2, which is within the reach of the ongoing DM indirect search experiments such as IceCube.
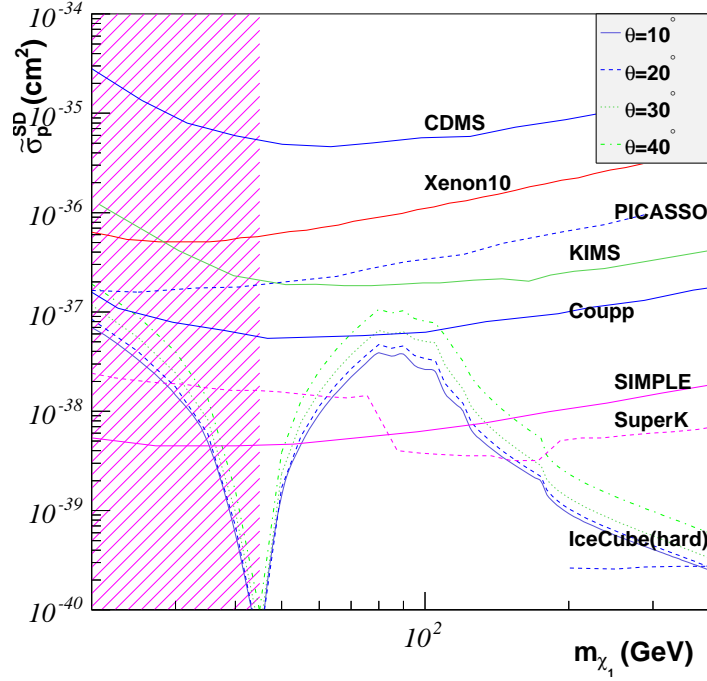
Acknowledgments

Figure 5: Effective spin-dependent cross section $\tilde{\sigma}_p^{SD}$ which is σ_p^{SD} rescaled by $r_\rho \approx r_\Omega$ for χ_1 elastically scattering off proton as function of the mass of χ_1. Four curves correspond to the mixing angle $\theta = 10°$(solid), $20°$(dashed), $30°$(dotted) and $40°$(dot-dashed) respectively. The current upper limits from various experiments such as KIMS [47], CDMS [48], Xenon10 [20], Coupp [49], Picasso [50], SIMPLE [51], SuperK [45], and IceCube [46] are also shown.

References

[1] P. H. Frampton, P. Q. Hung, and M. Sher, *Quarks and leptons beyond the third generation*, *Phys. Rept.* **330** (2000) 263, [`hep-ph/9903387`].

[2] M. Kobayashi and T. Maskawa, *CP Violation in the Renormalizable Theory of Weak Interaction*, *Prog. Theor. Phys.* **49** (1973) 652–657.

[3] W.-S. Hou, *CP Violation and Baryogenesis from New Heavy Quarks*, *Chin. J. Phys.* **47** (2009) 134, [`arXiv:0803.1234`].

[4] B. Holdom, *heavy quarks and electroweak symmetry breaking*, *Phys. Rev. Lett.* **57** (1986) 2496.

[5] J. Carpenter, R. Norton, S. Siegemund-Broka, and A. Soni, *properties of a composite higgs particle in a dynamically broken formulation of the standard model*, *Phys. Rev. Lett.* **65** (1990) 153–156.

[6] C. T. Hill, M. A. Luty, and E. A. Paschos, *Electroweak symmetry breaking by fourth generation condensates and the neutrino spectrum*, *Phys.Rev.* **D43** (1991) 3011–3025.

[7] P. Q. Hung and C. Xiong, *Renormalization Group Fixed Point with a Fourth Generation: Higgs-induced Bound States and Condensates*, *Nucl. Phys.* **B847** (2011) 160–178, [`arXiv:0911.3890`].

[8] R. Contino *Talk at Implications of LHC results for TEV-scale Physics, Aug.29-Sept.02l, CERN* (2011).

[9] The CDF collaboration, http://www-cdf.fnal.gov/physics/new/top/confNotes/tprime_CDFnotePub.pdf.

[10] **The CDF** Collaboration, T. Aaltonen *et. al.*, *Search for heavy bottom-like quarks decaying to an electron or muon and jets in $p\bar{p}$ collisions at $\sqrt{s} = 1.96$ TeV*, *Phys. Rev. Lett.* **106** (2011) 141803, [`arXiv:1101.5728`].

[11] A. Korytov *Talk at the EuroPhysics Conferences on High-Energy Physics (EPS2011), July.20-27, Grenoble, France* (2011).

[12] **Particle Data Group** Collaboration, K. Nakamura *et. al.*, *Review of particle physics*, *J. Phys.* **G37** (2010) 075021.

[13] H. Murayama, V. Rentala, J. Shu, and T. T. Yanagida, *Saving fourth generation and baryon number by living long*, `arXiv:1012.0338`.

[14] B. W. Lee and S. Weinberg, *Cosmological lower bound on heavy-neutrino masses*, *Phys. Rev. Lett.* **39** (1977) 165–168.

[15] E. W. Kolb and K. A. Olive, *The Lee-Weinberg Bound Revisited*, *Phys. Rev.* **D33** (1986) 1202. [Erratum-ibid.D34:2531,1986].

[16] M. W. Goodman and E. Witten, *Detectability of certain dark-matter candidates*, *Phys. Rev.* **D31** (1985) 3059.

[17] M. Srednicki, K. A. Olive, and J. Silk, *High-Energy Neutrinos from the Sun and Cold Dark Matter*, *Nucl. Phys.* **B279** (1987) 804.

[18] T. Falk, K. A. Olive, and M. Srednicki, *Heavy Sneutrinos as Dark Matter*, *Phys. Lett.* **B339** (1994) 248–251, [`hep-ph/9409270`].

[19] G. Belanger, A. Pukhov, and G. Servant, *Dirac Neutrino Dark Matter*, *JCAP* **0801** (2008) 009, [`arXiv:0706.0526`].

[20] J. Angle *et. al.*, *Limits on spin-dependent WIMP-nucleon cross-sections from the XENON10 experiment*, *Phys. Rev. Lett.* **101** (2008) 091301, [`arXiv:0805.2939`].

[21] W.-Y. Keung and P. Schwaller, *Long Lived Fourth Generation and the Higgs*, *JHEP* **06** (2011) 054, [`arXiv:1103.3765`].

[22] K. Enqvist, K. Kainulainen, and J. Maalampi, *cosmic abundances of very heavy neutrinos*, *Nucl. Phys.* **B317** (1989) 647–664.

[23] P. Langacker, *The Physics of Heavy Z-prime Gauge Bosons*, *Rev. Mod. Phys.* **81** (2009) 1199–1228, [`arXiv:0801.1345`].

[24] S. Baek, N. Deshpande, X. He, and P. Ko, *Muon anomalous g-2 and gauged L(muon) - L(tau) models*, *Phys.Rev.* **D64** (2001) 055006, [`hep-ph/0104141`].

[25] **Muon G-2 Collaboration** Collaboration, G. Bennett *et. al.*, *Final Report of the Muon E821 Anomalous Magnetic Moment Measurement at BNL*, *Phys.Rev.* **D73** (2006) 072003, [`hep-ex/0602035`]. Summary of E821 Collaboration measurements of the muon anomalous magnetic moment, each reported earlier in Letters or Brief Reports. Revised version submitted to Phys.Rev.D.

[26] K. Hagiwara, A. Martin, D. Nomura, and T. Teubner, *Improved predictions for g-2 of the muon and alpha(QED) (M**2(Z))*, *Phys.Lett.* **B649** (2007) 173–179, [`hep-ph/0611102`].

[27] M. S. Carena, A. Daleo, B. A. Dobrescu, and T. M. P. Tait, *Z-prime gauge bosons at the Tevatron*, *Phys. Rev.* **D70** (2004) 093009, [`hep-ph/0408098`].

[28] **for the CMS** Collaboration, V. Timciuc, *Search for High-Mass Resonances in the Dilepton Final State with the CMS Detector*, `arXiv:1111.4528`.

[29] A. Collaboration, *Search for dilepton resonances in pp collisions at sqrt(s) = 7 TeV with the ATLAS detector*, *Phys. Rev. Lett.* **107** (2011) 272002, [`arXiv:1108.1582`].

[30] **CMS** Collaboration, S. Chatrchyan *et. al.*, *Search for Resonances in the Dilepton Mass Distribution in pp Collisions at sqrt(s) = 7 TeV*, *JHEP* **05** (2011) 093, [`arXiv:1103.0981`].

[31] E. Accomando, A. Belyaev, L. Fedeli, S. F. King, and C. Shepherd-Themistocleous, *Z' physics with early LHC data*, Phys. Rev. **D83** (2011) 075012, [arXiv:1010.6058].

[32] J. Alwall, J. L. Feng, J. Kumar, and S. Su, *B's with Direct Decays: Tevatron and LHC Discovery Prospects in the bb+MET Channel*, arXiv:1107.2919.

[33] G. Belanger *et. al.*, *Indirect search for dark matter with micrOMEGAs2.4*, Comput. Phys. Commun. **182** (2011) 842–856, [arXiv:1004.1092].

[34] J. Erler and P. Langacker, *Precision Constraints on Extra Fermion Generations*, Phys. Rev. Lett. **105** (2010) 031801, [arXiv:1003.3211].

[35] K. Kainulainen, K. Tuominen, and J. Virkajarvi, *The WIMP of a Minimal Technicolor Theory*, Phys.Rev. **D75** (2007) 085003, [hep-ph/0612247].

[36] T. Asaka, S. Blanchet, and M. Shaposhnikov, *The nuMSM, dark matter and neutrino masses*, Phys. Lett. **B631** (2005) 151–156, [hep-ph/0503065].

[37] F. Bezrukov, H. Hettmansperger, and M. Lindner, *keV sterile neutrino dark matter in gauge extensions of the standard model*, Phys. Rev. **D81** (2010) 085032, [arXiv:0912.4415].

[38] R. Catena and P. Ullio, *A novel determination of the local dark matter density*, JCAP **1008** (2010) 004, [arXiv:0907.0018].

[39] G. Jungman, M. Kamionkowski, and K. Griest, *Supersymmetric dark matter*, Phys.Rept. **267** (1996) 195–373, [hep-ph/9506380].

[40] J. R. Ellis, A. Ferstl, and K. A. Olive, *Re-evaluation of the elastic scattering of supersymmetric dark matter*, Phys. Lett. **B481** (2000) 304–314, [hep-ph/0001005].

[41] **The CDMS-II Collaboration** Collaboration, Z. Ahmed *et. al.*, *Dark Matter Search Results from the CDMS II Experiment*, Science **327** (2010) 1619–1621, [arXiv:0912.3592].

[42] **XENON100 Collaboration** Collaboration, E. Aprile *et. al.*, *Dark Matter Results from 100 Live Days of XENON100 Data*, Phys.Rev.Lett. (2011) [arXiv:1104.2549].

[43] T. Cohen, D. J. Phalen, and A. Pierce, *On the Correlation Between the Spin-Independent and Spin-Dependent Direct Detection of Dark Matter*, Phys.Rev. **D81** (2010) 116001, [arXiv:1001.3408].

[44] M. Felizardo *et. al.*, *Final Analysis and Results of the Phase II SIMPLE Dark Matter Search*, `arXiv:1106.3014`.

[45] **Super-Kamiokande** Collaboration, S. Desai *et. al.*, *Search for dark matter WIMPs using upward through-going muons in Super-Kamiokande*, Phys. Rev. **D70** (2004) 083523, [`hep-ex/0404025`]. [Erratum-ibid.D70:109901,2004].

[46] **ICECUBE** Collaboration, R. Abbasi *et. al.*, *Limits on a muon flux from neutralino annihilations in the Sun with the IceCube 22-string detector*, Phys. Rev. Lett. **102** (2009) 201302, [`arXiv:0902.2460`].

[47] **KIMS** Collaboration, H. S. Lee *et. al.*, *Limits on WIMP-nucleon cross section with CsI(Tl) crystal detectors*, Phys. Rev. Lett. **99** (2007) 091301, [`arXiv:0704.0423`].

[48] **CDMS** Collaboration, D. S. Akerib *et. al.*, *Limits on spin-dependent WIMP nucleon interactions from the Cryogenic Dark Matter Search*, Phys. Rev. **D73** (2006) 011102, [`astro-ph/0509269`].

[49] E. Behnke *et. al.*, *Improved Limits on Spin-Dependent WIMP-Proton Interactions from a Two Liter CF_3I Bubble Chamber*, Phys. Rev. Lett. **106** (2011) 021303, [`arXiv:1008.3518`].

[50] S. Archambault *et. al.*, *Dark Matter Spin-Dependent Limits for WIMP Interactions on 19-F by PICASSO*, Phys. Lett. **B682** (2009) 185–192, [`arXiv:0907.0307`].

[51] M. Felizardo, T. Girard, T. Morlat, A. Fernandes, F. Giuliani, *et. al.*, *Final Analysis and Results of the Phase II SIMPLE Dark Matter Search*, `arXiv:1106.3014`.